arXiv:submit/3244116 [cs.CV] 25 Jun 2020

Space-Time Correspondence as a Contrastive Random Walk

Allan Jabri
UC Berkeley

Andrew Owens
University of Michigan

Alexei A. Efros
UC Berkeley

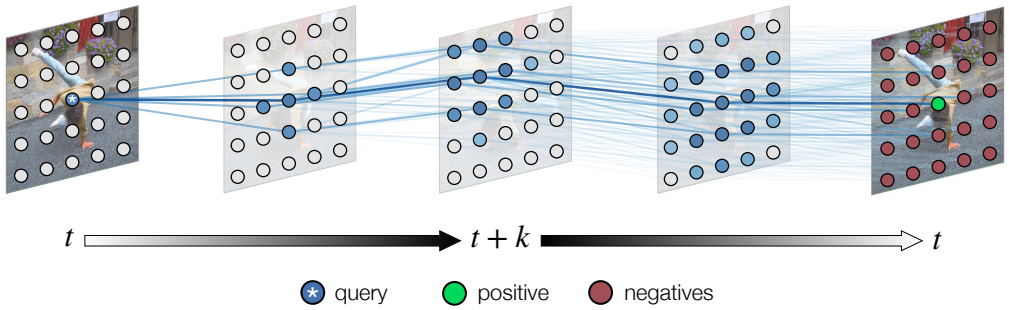

Figure 1: We represent video as a graph, where nodes are image patches, and edges are affinities (in some feature space) between nodes of neighboring frames. Our aim is to learn features such that temporal correspondences are represented by strong edges. We learn to find paths through the graph by performing a random walk between query and target nodes. A contrastive loss encourages paths that reach the target, implicitly supervising latent correspondence along the path. Learning proceeds *without labels* by training on a *palindrome* sequence, walking from frame t to $t+k$, then back to t, using the initial node itself as the target. Please see our webpage for videos.

Abstract

This paper proposes a simple self-supervised approach for learning representations for visual correspondence from raw video. We cast correspondence as link prediction in a space-time graph constructed from a video. In this graph, the nodes are patches sampled from each frame, and nodes adjacent in time can share a directed edge. We learn a node embedding in which pairwise similarity defines transition probabilities of a random walk. Prediction of long-range correspondence is efficiently computed as a walk along this graph. The embedding learns to guide the walk by placing high probability along paths of correspondence. Targets are formed without supervision, by cycle-consistency: we train the embedding to maximize the likelihood of returning to the initial node when walking along a graph constructed from a palindrome of frames. We demonstrate that the approach allows for learning representations from large unlabeled video. Despite its simplicity, the method outperforms the self-supervised state-of-the-art on a variety of label propagation tasks involving objects, semantic parts, and pose. Moreover, we show that self-supervised adaptation at test-time and edge dropout improve transfer for object-level correspondence.

1 Introduction

There has been a flurry of advances in self-supervised representation learning from still images, yet this has not translated into commensurate advances in learning from *video*. In the early days of computer vision, video was thought to be a simple extension of an image into time, to be modeled

Preprint. Under review.

by a spatio-temporal XYT volume [57, 95]. This view is now seeing a resurgence in the form of 3D convolutions [11], often used for tasks like action recognition. Yet, treating time as just another dimension is limiting [21]. One practical issue is the sampling rate mismatch between X and Y vs. T. But a more fundamental problem is that a physical point depicted at position (x, y) in frame t might not have any relation to what we find at that same (x, y) in frame $t + k$, as the object or the camera will have moved in arbitrary (albeit smooth) ways. This is why the notion of *temporal correspondence* — "what went where" [91] in a video — is so fundamental for learning from temporal visual data.

Recent self-supervision methods, such as those based on triplet losses and contrastive learning [80, 70, 92, 77, 31, 13], are effective for learning similarity between inputs when matching views (correspondences) are assumed to be known, e.g. formed by data augmentation. Temporal correspondences in video, however, are *latent*, and learning to find them leads to a chicken-and-egg problem: we need correspondences to train our model, yet we rely on our model to find these correspondences in the first place. An emerging line of work aims to address this problem by "bootstrapping" from an initially random representation, inferring which correspondences should be learned in a self-supervised manner e.g. via cycle-consistency of time [88, 84, 44]. While this is a promising direction, current methods rely on complex and greedy tracking procedures that may be susceptible to local optima, especially when applied recurrently in time.

In this paper, we learn a representation for temporal correspondence by formulating the problem as probabilistic pathfinding on a graph. The graph is constructed from a video, where nodes are image patches and only nodes in neighboring frames share an edge. The strength of the edge is determined by a learned similarity function, whose aim is to place large weight along paths linking visually corresponding patches (see Figure 1). Inspired by Meila and Shi [53], we capture global connectivity in the graph by modeling local transition probabilities of a random walker stepping through time. Our learning problem requires supervision — namely, the target that the walker should aim for. In lieu of ground truth labels, we use the idea of cycle-consistency [99, 88, 84], by turning training videos into *palindromes*, where the first half is repeated backwards. This provides every path with a target — getting back to its starting point. With this formulation, we can view each step of the random walker as a contrastive learning problem [60], where the walker's target provides supervision for the entire chain of intermediate steps.

The central benefit of the proposed model is that it efficiently considers many possible paths through the graph by simply computing the expected outcome of a random walk. This allows the model to obtain a useful learning signal from all patches in the video simultaneously, and overcome ambiguity to learn from harder examples encountered during training. Despite its simplicity, the method learns a representation that is effective for a variety of correspondence tasks, without any additional adaptation. We obtain results that outperform state-of-the-art self-supervised methods on video object segmentation, pose keypoint propagation, and semantic part propagation. The model scales effectively, obtaining improvements in performance as the length of the random walks used for training increases. We also show several extensions of the model that further improve the quality of its correspondences for object segmentation, including test-time adaptation, and an edge dropout [73] technique that encourages the model to group "common-fate" [90] nodes together.

2 Contrastive Random Walks on Video

We represent each video as a directed graph where nodes are patches, and weighted edges connect nodes in neighboring frames. Let $\mathbf{I}$ be a set of frames of a video and $\mathbf{q}_t$ be the set of N nodes extracted from frame $\mathbf{I}_t$, e.g. by sampling overlapping patches in a grid. An encoder ϕ maps nodes to l_2-normalized d-dimensional vectors, which we use to compute a pairwise similarity function $d_\phi(q_1, q_2) = \langle \phi(q_1), \phi(q_2) \rangle$ and an embedding matrix for $\mathbf{q}_t$ denoted $Q_t \in \mathbb{R}^{N \times d}$. We convert pairwise similarities into non-negative affinities by applying a softmax (with temperature τ) over edges departing from the node. For two adjacent timesteps t and $t + 1$, the stochastic matrix of affinities is

$$A_t^{t+1}(i, j) = \texttt{softmax}(Q_t Q_{t+1}^\top)_{ij} = \frac{\exp(d_\phi(\mathbf{q}_t^i, \mathbf{q}_{t+1}^j)/\tau)}{\sum_l \exp(d_\phi(\mathbf{q}_t^i, \mathbf{q}_{t+1}^l)/\tau)}, \tag{1}$$

where the `softmax` is row-wise. Note that this describes only the *local* affinity between the patches of two video frames, $\mathbf{q}_t$ and $\mathbf{q}_{t+1}$. The affinity matrix for the entire graph, which relates all nodes in the video as a Markov chain, is sparse and composed of local affinity matrices.

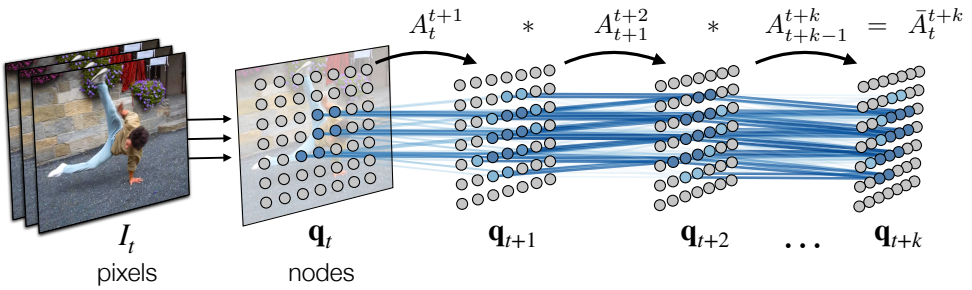

Figure 2: **Correspondence as a Random Walk**. We build a space-time graph by extracting nodes from each frame and allowing directed edges between nodes in neighbouring frames. The transition probabilities of a random walk along this graph are determined by learned pairwise node similarity.

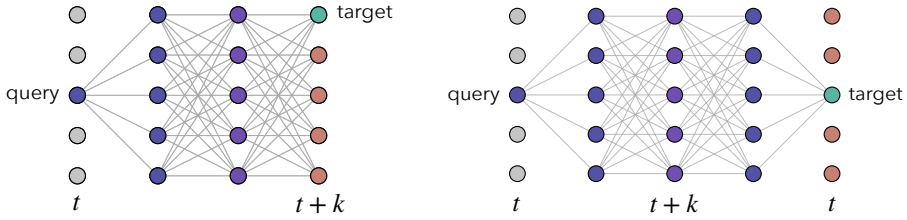

Figure 3: **Learning to Walk on Video.** (a) Specifying a target multiple steps in the future provides implicit supervision for *latent* correspondences along each path *(left)*. (b) We can construct targets for free by choosing palindromes as sequences for learning *(right)*.

Given the spatio-temporal connectivity of the graph, a step of a random walker on this graph can be seen as performing probabilistic tracking by *contrasting* similarity of neighboring nodes (using ϕ). Let X_t be the state of the walker at time t, with transition probabilities $A_t^{t+1}(i,j) = P(X_{t+1} = j | X_t = i)$, where $P(X_t = i)$ is the probability of being at node i at time t. With this view, we can formulate long-range correspondence as walking multiple steps along the graph (Figure 2). We chain the transitions to obtain the distribution over nodes after k steps:

$$\bar{A}_t^{t+k} = \prod_{i=0}^{k-1} A_{t+i}^{t+i+1} = P(X_{t+k} | X_t). \tag{2}$$

Guiding the walk. Our aim is to train the embedding to encourage the random walker to follow paths of corresponding patches as it steps through time. While ultimately we will train without labels, for motivation suppose that we did have ground-truth correspondence labels between nodes in two frames of a video, t and $t+k$ (Figure 3a). We could use these labels to fit the embedding by maximizing the probability that a random walk beginning at a *query* node at t ends at the *target* node at time $t+k$:

$$\mathcal{L}_{sup} = \mathcal{L}_{CE}(\bar{A}_t^{t+k}, Y_t^{t+k}) = -\sum_{i=1}^{N} \log P(X_{t+k} = Y_t^{t+k}(i) | X_t = i), \tag{3}$$

where $\mathcal{L}_{CE}$ is cross entropy loss and Y_t^{t+k} are correspondence labels for matching time t to $t+k$. Under this formulation, the walk can be viewed as a chain of contrastive learning problems. Providing supervision at *every* step amounts to maximizing similarity between the embeddings of query and target nodes adjacent in time, while minimizing similarity to embeddings of all other neighbors.

The more interesting case is supervision of long-range correspondence, i.e. when $k > 1$. In this case, the labels of t and $t+k$ provide *implicit* supervision for intermediate frames $t+1, ..., t+k-1$, assuming that latent correspondences exist to link t and $t+k$. Recall that in computing $P(X_{t+k}|X_t)$, we marginalize over all intermediate paths that link nodes in t and $t+k$. By minimizing $\mathcal{L}_{sup}$, we shift weight to paths that link the query and target. In relatively easy cases (e.g. smooth videos with no occlusions) the paths that the walker takes from each node will not overlap, and these paths will simply be reinforced. In harder cases, such as where deformation or multi-modality make correspondence ambiguous, the transitions will be split over multiple latent correspondences, such

that we consider a distribution over paths. The embedding captures similarity between nodes in a manner that allows for hedging probability over paths to overcome ambiguity, while avoiding transitions to nodes that lead the walker astray.

Self-supervision with palindromes. How can we identify query-target pairs that are known to correspond, without human supervision? We can consider training on graphs in which correspondence between the first and last frames are known, by construction. One such class of sequences are *palindromes*, i.e. sequences that are unchanged when reversed, for which correspondence is known since the first and last frames are identical. Given a sequence of frames $(I_t, ..., I_{t+k})$, we form the palindrome by simply concatenating the sequence with a temporally reversed version of itself: $(I_t, ...I_{t+k}, ...I_t)$. Treating each query node's position as its own target (Figure 3b), we obtain the following cycle-consistency objective, where the ground truth labels, I, are the identity matrix:

$$\mathcal{L}^k_{cyc} = \mathcal{L}_{CE}(\bar{A}^{t+k}_t \bar{A}^t_{t+k}, I) = -\sum_{i=1}^{N} \log P(X_{t+2k} = i | X_t = i) \tag{4}$$

This self-supervised formulation enables learning correspondences over multiple frames from raw video. The model computes a distribution over soft matches at every time step, allowing backpropagation over all paths through the graph during training. This allows the model to consider long-range correspondences, and also to consider and eventually learn possible matches that are dissimilar in local appearance but nonetheless may correspond.

Contrastive learning with latent views. To help explain why this model learns a useful representation, we can interpret it as contrastive learning with latent views. A standard contrastive learning formulation brings two views of the same example together by learning a representation that minimizes the loss $\mathcal{L}_{CE}(U^2_1, I)$ [60], where $U^2_1 \in \mathbb{R}^{n \times n}$ is the matrix of pairwise dot products between the vectors of the first and second views of n examples, converted into a stochastic matrix by softmax as in Equation 1. Suppose, however, that we do not know *which* views should be matched with one another — merely that there should be a soft one-to-one correspondence between them. This can be formulated as contrastive learning guided by a cycle-consistency constraint: each image chooses from among the possible distractors, composing U^2_1 with the "transposed" stochastic matrix U^1_2 of similarities between the second and first view. This produces the loss $\mathcal{L}_{contrast} = \mathcal{L}_{CE}(U^2_1 U^1_2, I)$, which is akin to the cycle walk loss of Equation 4. In this work, we chain contrastive predictions between latent views to form a cycle of multiple steps in the embedding space, which makes for a more challenging self-supervision task due to compounding error.

2.1 Edge Dropout

Beyond correspondences of image patches, one could also consider correspondence on the level of broader *segments*, where points within a segment have strong affinity to all other points in the segment. This inspires a trivial extension of our method– randomly dropping edges from the graph, thereby forcing the walker to consider alternative paths. We apply dropout [73] (with rate δ) to the transition matrix A to obtain $\tilde{A} = \texttt{dropout}(A, \delta)$ and then renormalize. The resulting transition matrix B and noisy cycle loss are:

$$B_{ij} = \frac{\tilde{A}_{ij}}{\sum_l \tilde{A}_{il}} \qquad \mathcal{L}^k_{c\tilde{y}c} = \mathcal{L}_{CE}(B^t_{t+k} B^{t+k}_t, I). \tag{5}$$

Edge dropout affects the task by randomly obstructing paths, thus encouraging hedging of mass to paths highly correlated with the ideal path, similar to the effect in spectral-based segmentation [72, 53]. We will see in Section 3.2 that edge dropout improves transfer to object-level correspondence tasks.

2.2 Implementation

We now describe in detail how we construct the graph, and how we parameterize the node embedding ϕ. Algorithm 1 provides complete pseudocode for the method.

Pixels to Nodes. At training time, we follow [34], where patches of size 64×64 are sampled on a 7×7 grid from a 256×256 image (i.e. 49 nodes per frame). Patches are spatially jittered to prevent matching based on borders. At test time, we found that we could reuse the convolutional feature map between patches instead of processing the patches independently [46], making the features computable with only a single feed-forward pass of our network.[1]

[1] Despite our best efforts, we found that using a single convolutional feature map at training left the learning algorithm susceptible to learning shortcut solutions. We provide more details in Section B.

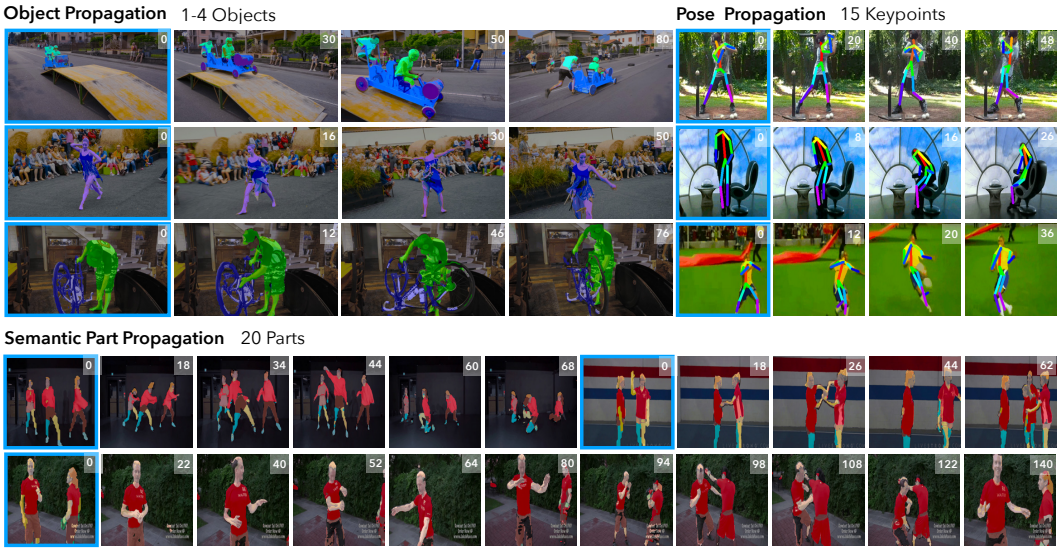

Figure 4: Qualitative results for label propagation under our model for object, pose, and semantic part propagation tasks. The first frame is indicate with a blue outline. **Please see our webpage for video results**, as well as a qualitative comparison with other methods.

Encoder ϕ. We create an embedding for each image patch using a convolutional network, namely ResNet-18 [33]. Following common practice in similarity learning [31], we apply a linear projection and l_2 normalization after the average pooling layer, obtaining a 128-dimensional vector.

Subcycles. During training, we consider cycles of multiple lengths. For a sequence of length T, we optimize all subcycles: $\mathcal{L}_{train} = \sum_{i=1}^{T} \mathcal{L}_{cyc}^{i}$. This loss encourages the sequence of nodes visited in the walk to be a palindrome, i.e. on a walk of length N, the node visited at step t should be the same node as $N - t$. It also leads to a natural training curriculum, as short walks are easier to learn than long ones. These additional losses can be computed efficiently, since they share the same affinity matrices (Equation 1).

Algorithm 1 Pseudocode in a PyTorch-like style.

```
# load a minibatch x with B sequences
for x in loader:
  # Split image into patches
  # B x C x T x H x W -> B x C x T x P x h x w
  x = unfold(x, (patch_size, patch_size))
  x = spatial_jitter(x)
  # Embed patches (B x C x T x P)
  v = l2_norm(resnet(x))

  # Transitions from t to t+1 (B x T x P x P)
  A = bmm(v[:,:,:-1], v[:,:,1:]) / temperature

  # Transition similarities for palindrome graph
  AA = cat((A, A[:,::-1].transpose(-1,-2), 1)

  # Walk
  At = eye(P)
  for t in range(2*T):
   At = bmm(softmax(dropedge(AA[:,t]),dim=-1), At)

  # Target is the original node (Equation 4)
  loss = cross_ent_loss(At, labels=[range(P)]*B)
  loss.backward()
```

`bmm`: batch matrix multiplication; `eye`: identity matrix; `cat`: concatenation.

Training. We train ϕ using the (unlabeled) videos from Kinetics [11], with Algorithm 1. We used the Adam optimizer [39] for one million updates, with 24 sequences per batch and a learning rate of 10^{-4}. We use a temperature of $\tau = 0.07$ in Equation 1, following [92] and resize frames to 256×256 (before extracting nodes as above). Except when indicated otherwise, we set edge dropout to 0. While we trained the model with 24-sequence batches split over three 1080Ti GPUs, we were able to train the model on a single GPU (with batch size 8).

3 Experiments

We demonstrate that the learned representation is effective for dense label propagation tasks, ablate the effects of edge dropout and training sequence length, and evaluate self-supervised adaptation at test-time. Please find additional comparisons to supervised methods, ablations and qualitative results in the Appendix.

3.1 Transferring the Learned Representation

We apply the trained embedding on label propagation tasks involving objects, semantic parts, and human pose. To isolate the effect of the representation, we use a simple algorithm for inference. Qualitative results are shown in Figure 4.

Method	Resolution	Train Data	$\mathcal{J}\&\mathcal{F}_\text{m}$	$\mathcal{J}_\text{m}$	$\mathcal{J}_\text{r}$	$\mathcal{F}_\text{m}$	$\mathcal{F}_\text{r}$
ImageNet [33]	1×	ImageNet	62.1	59.8	68.3	64.4	72.4
MoCo [31]	1×	ImageNet	60.1	57.1	66.0	63.1	71.9
VINCE [25]	1×	Kinetics	60.4	57.9	66.2	62.8	71.5
CorrFlow [43]	2×	OxUvA	50.3	48.4	53.2	52.2	56.0
MAST [42]	2×	OxUvA	63.7	61.2	73.2	66.3	78.3
MAST [42]	2×	YT-VOS	65.5	63.3	73.2	67.6	77.7
Colorization [83]	1×	Kinetics	34.0	34.6	34.1	32.7	26.8
TimeCycle [88]	1×	VLOG	48.7	46.4	50.0	50.0	48.0
UVC [44]	1×	Kinetics	58.1	56.8	65.7	59.5	65.1
UVC+track [44]	1×	Kinetics	59.5	57.7	68.3	61.3	69.8
Ours	1×	Kinetics	**66.1**	**63.8**	**74.9**	**68.7**	**80.9**
w/ dropout	1×	Kinetics	67.6	64.8	76.1	70.2	82.1
w/ dropout & test-time training	1×	Kinetics	68.3	65.5	78.6	71.0	82.9

Table 1: **Video object segmentation results on DAVIS 2017 val set** Comparison of our method (3 variants), with previous self-supervised approaches and strong image representation baselines. *Resolution* indicates if the approach uses a high-resolution (2x) feature map. *Train Data* indicates which dataset was used for pre-training. $\mathcal{F}$ is a boundary alignment metric, while $\mathcal{J}$ measures region similarity as IOU between masks. Comparison to supervised methods can be found in Section A.

Label Propagation. All evaluation tasks considered can be cast as video label propagation, where the task is to predict labels for each pixel in *target* frames of a video given only ground-truth for the first frame (i.e. the *source*). We use the model as a similarity function for prediction by k-nearest neighbors, which is natural under our model and follows prior work for fair comparison [88, 44]. Say we are given source nodes $\mathbf{q}_s$ with labels $L_s \in \mathbb{R}^{N \times C}$, and target nodes $\mathbf{q}_t$. Let K_t^s be the matrix of transitions between $\mathbf{q}_t$ and $\mathbf{q}_s$ (Equation 1), with the special property that only the top$-k$ transitions are considered per source node. Then, labels L_t are propagated as $L_t = K_t^s L_s$ where each row corresponds to the soft distribution over labels for a node, predicted by k-nearest neighbor under d_ϕ. Following common practice [88, 43, 44], we use a queue of context frames and restrict the set of source nodes considered to be within a spatial neighborhood of the query node for efficiency. The source set includes nodes of the first labeled frame, as well as the nodes in previous m frames, whose predicted labels are used for auto-regressive propagation.

Baselines. We compare to a variety of methods, all of which use ResNet-18 [32] as the network backbone. First, we consider strong image- and video-based representation learning methods. Following the setup in [88] and for consistency across methods (including our own), we use the features in the last convolutional feature map as node embeddings at test-time. We consider a strong supervised training method, a model trained on **ImageNet** [16]. We also consider a strong self-supervised method, **MoCo** [31], due to state-of-the-art performance, code availability, efficiency of training. Finally, we compare with the video-based contrastive learning method, **VINCE** [25], which extends MoCo to videos (Kinetics) with views from data augmentation *and* neighbors in time.

We also compare with state-of-the-art self-supervised temporal correspondence approaches. **Wang et al.** [88] uses cycle-consistency to train a spatial transformer as a deterministic patch tracker. We also consider methods based on the **Colorization** approach of Vondrick et al. [83], including high-resolution methods: **CorrFlow** [43] and **MAST** [42]. CorrFlow combines cycle consistency with colorization. MAST uses a deterministic region localizer and memory bank for high-resolution colorization, and performs multi-stage training on [79]. Notably, both methods use feature maps that are significantly higher resolution than other approaches (2×), which they implement by removing the initial pooling layer of ResNet. Finally, **UVC** [44] jointly optimizes losses for colorization, grouping, pixel-wise cycle-consistency, and patch tracking with a deterministic patch localizer.

3.1.1 Video Object Segmentation

We evaluate our model on DAVIS 2017 [67], a popular benchmark for video object segmentation. We consider the semi-supervised setting, which involves multi-object (i.e. 2-4) label propagation. Following common practice, we evaluate on 480p resolution images and use $k = 5, m = 8$. We report mean (m) and recall (r) of standard boundary alignment ($\mathcal{F}$) and region similarity ($\mathcal{J}$) metrics, detailed in [64].

As shown in Table 1, our approach outperforms all other self-supervised methods, without relying on machinery such as localization modules or multi-stage training. Our method gives a relative improvement of 15% compared to state-of-the-art methods that train on Kinetics. We also outperform [42] despite being more simple at train and test time, and using a lower-resolution feature map. Moreover, we perform better than state-of-the-art image-level self-supervised learning approaches MoCo [31] and VINCE [25], suggesting that for tasks that involve dense similarity, it may not be optimal to choose views for contrastive learning by random crop data augmentation of neighboring frames. Finally, we perform competitively with many of the supervised methods with architectures specially designed for dense tracking [64, 10, 85]; details can be found in Section A.

3.1.2 Pose Tracking

We consider pose tracking on the JHMDB benchmark, which involves tracking 15 keypoints. We follow the evaluation protocol of [44], using 320×320px images and $m = 7$ frames of context. As seen in Table 2, our model outperforms the self-supervised state-of-the-art, including video colorization models that directly optimize for fine-grained matching with pixel-level objectives [44]. We attribute this success to the fact that our model sees sufficient hard negative samples drawn from the same image at training time to learn discriminative correspondence.

3.1.3 Video Part Segmentation

We consider the semantic part segmentation task of the Video Instance Parsing (VIP) benchmark [98], which involves propagating labels of 20 parts — such as arm, leg, hair, shirt, hand — requiring more precise correspondence than DAVIS. The sequences are longer and sampled at a lower frame rate. We follow the evaluation protocol of [44], using 560×560px images and $m = 1$. We outperform the self-supervised state-of-the-art, and when using more temporal context (i.e. $m = 4$), we outperform the benchmark's supervised approach [98].

	Parts	Pose	
Method	mIoU	PCK@0.1	PCK@0.2
TimeCycle [88]	28.9	57.3	78.1
UVC [44]	34.1	58.6	79.6
Ours	36.0	59.0	83.2
Ours + context	**38.6**	**59.3**	**84.9**
ResNet-18 [32]	31.9	53.8	74.6
ATEN [98]	**37.9**	–	–
Yang et al. [93]	–	**68.7**	**92.1**

Table 2: **Part and Pose Propagation tasks**, with the VIP and JHMDB benchmarks, respectively. For comparison, we show supervised methods below.

3.2 Variations of the Model

Edge dropout. We test the hypothesis (Figure 5b) that edge dropout should improve performance on the object segmentation task, by training our model with different edge dropout rates: {0, 0.1, 0.2, 0.3, 0.4}. We find that small amounts of dropout provide a significant improvement on the downstream DAVIS benchmark. We hypothesize that edge dropout simulates occasional partial occlusion, forcing the network to form alternate matches if necessary.

Path length. We also asked how important it is for the model to perform its random walk over long temporal distances during training, by using clips of length 2, 4, 6, or 10 (resulting in paths of length 4, 8, 12, or 20). Longer sequences make for harder tasks due to compounding error. We found that longer training sequences results in accelerated convergence as well as improved performance on the DAVIS task (Figure 5c). This is in contrast to prior work [88]; we attribute this success to considering multiple paths at training time, which allows for tracking along and thus learning from long sequences, despite ambiguity.

Performance as function of training time We found that the model's downstream performance on DAVIS improves as more data is seen during self-supervised training (Figure 5a). In contrast to Wang et al [88], there is no evidence of saturation of performance on the downstream task.

3.3 Test-time Training

A key benefit of self-supervised learning is that, because there is no reliance on labeled data, training need not be limited to the training phase, but can continue during deployment [3, 56, 75]. Our approach is especially suited for such adaptation, given the non-parametric inference procedure. We ask whether the model can improve its ability to find object correspondences by fine-tuning the embedding *at test time* on a novel video. Given an input video, we can perform a small number of iterations of gradient descent on the self-supervised loss (Algorithm 1) *prior* to label propagation.

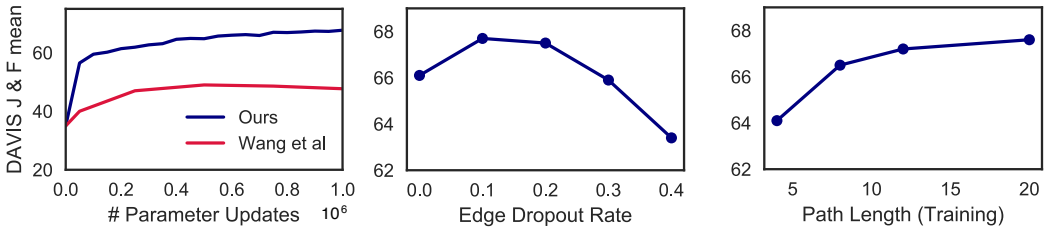

(a) performance vs. training time (b) effect of edge dropout (c) effect of path length

Figure 5: **Variations of the Model.** (a) Downstream task performance as a function of training time. (b) Moderate edge dropout improves object-level correspondences. (c) Training on longer paths is beneficial. All evaluations are on the DAVIS segmentation task.

We argue it is most natural to consider an online setting, where the video is ingested as a stream and fine-tuning is performed continuously on the sliding window of k frames around the current frame. Note that only the raw, unlabeled video is used for this adaptation; we do not use the provided label mask. As seen in Table 1, test-time training gives an improvement on the video object segmentation task. Interestingly, we see most improvement (+2.5%) in the recall of the region similarity metric $\mathcal{J}_{recall}$ (which measures how often more than 50% of the object is segmented). More experiment details can be found in Section E.

4 Related Work

Temporal Correspondence. Many early methods represented video as a spatio-temporal XYT volume, where patterns, such as lines or statistics of spatio-temporal gradients, were computed for tasks like gait tracking [57] and action recognition [95]. Because the camera was usually static, this provided an implicit temporal correspondence via (x, y) coordinates. For more complex videos, optical flow [48] was used to obtain short-range explicit correspondences between patches of neighboring frames. However, optical flow proved too noisy to provide long-range composite correspondences across many frames. Object tracking was meant to offer robust long-range correspondences for a given tracked object. But after many years of effort (see [22] for overview), that goal was largely abandoned as too difficult, giving rise to "tracking as repeated detection" paradigm [68], where trained object detectors are applied to each frame independently. In the case of multiple objects, the process of "data association" connects these detections into coherent object tracks. Data association is often cast as an optimization problem for finding paths through video that fulfill certain constraints, e.g. appearance, position overlap, etc. This can be addressed in a variety of ways, including dynamic programming, particle filtering, various graph-based combinatorial optimization, and more recently, graph neural networks [96, 69, 6, 66, 12, 94, 38, 37, 40, 9]. Our work can be thought of as performing soft, contrastive data association directly on pixels, as a means for representation learning.

Graph Partitioning and Graph Representation Learning. Graphs have also been widely used in image and video segmentation. Given a video, a graph would be formed by connecting pixels in spatio-temporal neighborhoods, followed by spectral clustering [71, 72, 23] or MRF/GraphCuts [8]. Most relevant to us is work of Meila and Shi [53], which posed Normalized Cuts as a Markov random walk, describing an algorithm for learning an affinity function by fitting the transition probabilities to be uniform within segments and zero otherwise. While above methods solve for connectivity given fixed nodes, graph representation learning approaches solve for node representations given fixed connectivity [29]. Most related, similarity learning approaches define neighborhoods of positives with fixed (i.e. k-hop neighborhood) or stochastic (i.e. random walk) heuristics [65, 27, 76], while sampling negatives at random. Backstrom et al. [4] learns to predict links by supervising a random walk on social network data. Likewise, we learn to predict links between patches in a video, but do so to learn a representation and supervise the walker with cycle-consistency.

Visual Representation with Self-Supervision. Most work in self-supervised representation learning can be interpreted as data imputation: given an example, the task is to predict a part — or *view* — of its data given another view [5, 15, 14]. Earlier work leveraged unlabeled visual datasets by constructing *pretext* prediction tasks [17, 58, 97]. For video, temporal information makes for natural pretext tasks, including future prediction [26, 74, 52, 47, 50], arrow of time [55, 89], motion estimation [1, 36, 78, 45] or audio [62, 2, 61, 41]. The use of off-the-shelf tracking to provide supervisory signal for learning visual similarity has also been explored [86, 87, 63]. Recent progress

in self-supervised learning has focused on improving techniques for large-scale distance learning, e.g. by combining the cross-entropy loss with negative sampling [28, 54]. Sets of views are formed by composing various data augmentations of the same instance [18, 7, 92], with domain knowledge being crucial for picking the right data augmentations. Strong image-level visual representations can be learned by heuristically choosing views that are close in space [80, 31, 13], in time [70, 30, 25] or both [35, 77], even when relying on noisy negative samples. However, forcing neighboring frames or crops to be similar is not always desirable because they may not be in correspondence. In contrast, we adaptively choose which pairs of crops to bring closer, which amounts to a sort of automatic view selection.

Self-supervised Correspondence and Cycle-consistency in Time Our approach is directly inspired by recent work that uses cycle-consistency [99, 19] in time as supervisory signal for learning visual representations from video [88, 84]. The key idea is to use self-supervised tracking as a pretext task: given a patch, first track forward in time, then backward, with the aim of ending up where it started, forming a cycle. At training, these methods rely on deterministic trackers in a greedy manner, which limits them to sampling, and learning from, one path at a time. In contrast, our approach maintains a distribution over matches at every time step, allowing us to assign credit over many paths to obtain a dense learning signal and overcome ambiguity. Li et al. [44] considers only pairs of frames, combining patch tracking with other losses including color label propagation [83], spatial concentration, and cycle-consistency via an orthogonality constraint [24]. Recently, Lai et al. [43, 42], inspired by [83], explore and improve architectural design decisions that yield impressive results on video object segmentation and tracking tasks. While colorization is a useful cue, the underlying assumption that corresponding pixels have the same color is often violated, e.g. due to changes in lighting or deformation. In contrast, our loss permits correspondences between image regions that may have significant differences in their appearance.

5 Discussion

We presented a simple approach for learning representations for correspondence from raw video, based on training a random walker to walk along cycles on a space-time graph. Despite its simplicity, the method achieves state-of-the-art performance among self-supervised methods on video object segmentation, and part and pose propagation. We view this work as a step toward scaling up self-supervised representation learning to the challenges of large-scale unlabelled video data, including gracefully adapting to new data in an online manner. Moreover, we hope this paper provides insight for further study of representation learning with latent positives.

6 Broader Impact

Research presented in the paper has a potential to positively contribute to a number of practical applications where establishing temporal correspondence in video is critical, among them pedestrian safely in automotive settings, patient monitoring in hospitals and elderly care homes, video-based animal monitoring and 3D reconstruction, etc. However, there is also a potential for the technology to be used for nefarious purposes, mainly in the area of unauthorized surveillance, especially by autocratic regimes. As partial mitigation, we commit to not entering into any contracts involving this technology with any government or quasi-governmental agencies of countries with an *EIU Democracy Index* [20] score of 4.0 or below ("authoritarian regimes"), or authorizing them to use our software.

Acknowledgments We thank Amir Zamir, Ashish Kumar, Tim Brooks, Bill Peebles, Dave Epstein, Armand Joulin, and Jitendra Malik for very helpful feedback. We are also grateful to the wonderful members of VGG group for hosting us during a dreamy semester at Oxford. This work would not have been possible without the hospitality of Port Meadow and the swimming pool on Iffley Road. Research was supported, in part, by NSF grant IIS-1633310, the DARPA MCS program, and NSF IIS-1522904. AJ is supported by the PD Soros Fellowship.

References

[1] Pulkit Agrawal, Joao Carreira, and Jitendra Malik. Learning to see by moving. In *ICCV*, 2015.

[2] Relja Arandjelovic and Andrew Zisserman. Look, listen and learn. In *Proceedings of the IEEE International Conference on Computer Vision*, pages 609–617, 2017.

[3] Michal Irani Assaf Shocher, Nadav Cohen. "zero-shot" super-resolution using deep internal learning. In *The IEEE Conference on Computer Vision and Pattern Recognition (CVPR)*, June 2018.

[4] Lars Backstrom and Jure Leskovec. Supervised random walks: predicting and recommending links in social networks. In *Proceedings of the fourth ACM international conference on Web search and data mining*, pages 635–644, 2011.

[5] Suzanna Becker and Geoffrey E Hinton. Self-organizing neural network that discovers surfaces in random-dot stereograms. *Nature*, 355(6356):161–163, 1992.

[6] Jerome Berclaz, Francois Fleuret, Engin Turetken, and Pascal Fua. Multiple object tracking using k-shortest paths optimization. *IEEE transactions on pattern analysis and machine intelligence*, 33(9):1806–1819, 2011.

[7] Piotr Bojanowski and Armand Joulin. Unsupervised learning by predicting noise. In *Proceedings of the 34th International Conference on Machine Learning-Volume 70*, pages 517–526. JMLR. org, 2017.

[8] Yuri Boykov and Gareth Funka-Lea. Graph cuts and efficient nd image segmentation. *International journal of computer vision*, 70(2):109–131, 2006.

[9] Guillem Brasó and Laura Leal-Taixé. Learning a neural solver for multiple object tracking. In *Proceedings of the IEEE/CVF Conference on Computer Vision and Pattern Recognition*, pages 6247–6257, 2020.

[10] Sergi Caelles, Kevis-Kokitsi Maninis, Jordi Pont-Tuset, Laura Leal-Taixé, Daniel Cremers, and Luc Van Gool. One-shot video object segmentation. In *CVPR*, 2017.

[11] Joao Carreira and Andrew Zisserman. Quo vadis, action recognition? a new model and the kinetics dataset. In *Computer Vision and Pattern Recognition (CVPR)*, 2017.

[12] Albert YC Chen and Jason J Corso. Temporally consistent multi-class video-object segmentation with the video graph-shifts algorithm. In *2011 IEEE Workshop on Applications of Computer Vision (WACV)*, pages 614–621. IEEE, 2011.

[13] Ting Chen, Simon Kornblith, Mohammad Norouzi, and Geoffrey Hinton. A simple framework for contrastive learning of visual representations. *arXiv preprint arXiv:2002.05709*, 2020.

[14] Sumit Chopra, Raia Hadsell, and Yann LeCun. Learning a similarity metric discriminatively, with application to face verification. In *2005 IEEE Computer Society Conference on Computer Vision and Pattern Recognition (CVPR'05)*, volume 1, pages 539–546. IEEE, 2005.

[15] Virginia R de Sa. Learning classification with unlabeled data. In *Advances in neural information processing systems*, pages 112–119, 1994.

[16] Jia Deng, Wei Dong, Richard Socher, Li-Jia Li, Kai Li, and Li Fei-Fei. Imagenet: A large-scale hierarchical image database. In *Computer Vision and Pattern Recognition (CVPR)*, 2009.

[17] Carl Doersch, Abhinav Gupta, and Alexei A. Efros. Unsupervised visual representation learning by context prediction. In *ICCV*, 2015.

[18] Alexey Dosovitskiy, Philipp Fischer, Jost Tobias Springenberg, Martin Riedmiller, and Thomas Brox. Discriminative unsupervised feature learning with exemplar convolutional neural networks. *IEEE transactions on pattern analysis and machine intelligence*, 38(9):1734–1747, 2015.

[19] Debidatta Dwibedi, Yusuf Aytar, Jonathan Tompson, Pierre Sermanet, and Andrew Zisserman. Temporal cycle-consistency learning. In *Proceedings of the IEEE Conference on Computer Vision and Pattern Recognition*, pages 1801–1810, 2019.

[20] EIU.com. Democracy index 2019 a year of democratic setbacks and popular protest. https://www.eiu.com/public/topical_report.aspx?campaignid=democracyindex2019, 2019.

[21] Christoph Feichtenhofer, Haoqi Fan, Jitendra Malik, and Kaiming He. Slowfast networks for video recognition. In *Proceedings of the IEEE International Conference on Computer Vision*, pages 6202–6211, 2019.

[22] David A. Forsyth and Jean Ponce. *Computer Vision - A Modern Approach, Second Edition.* Pitman, 2012.

[23] Charless Fowlkes, Serge Belongie, Fan Chung, and Jitendra Malik. Spectral grouping using the nystrom method. *IEEE transactions on pattern analysis and machine intelligence*, 26(2):214–225, 2004.

[24] Leon A Gatys, Alexander S Ecker, and Matthias Bethge. A neural algorithm of artistic style. *arXiv preprint arXiv:1508.06576*, 2015.

[25] Daniel Gordon, Kiana Ehsani, Dieter Fox, and Ali Farhadi. Watching the world go by: Representation learning from unlabeled videos, 2020.

[26] Ross Goroshin, Joan Bruna, Jonathan Tompson, David Eigen, and Yann LeCun. Unsupervised learning of spatiotemporally coherent metrics. *ICCV*, 2015.

[27] Aditya Grover and Jure Leskovec. node2vec: Scalable feature learning for networks. In *Proceedings of the 22nd ACM SIGKDD international conference on Knowledge discovery and data mining*, pages 855–864, 2016.

[28] Michael Gutmann and Aapo Hyvärinen. Noise-contrastive estimation: A new estimation principle for unnormalized statistical models. In *Proceedings of the Thirteenth International Conference on Artificial Intelligence and Statistics*, pages 297–304, 2010.

[29] William L Hamilton, Rex Ying, and Jure Leskovec. Representation learning on graphs: Methods and applications. *arXiv preprint arXiv:1709.05584*, 2017.

[30] Tengda Han, Weidi Xie, and Andrew Zisserman. Video representation learning by dense predictive coding. In *Proceedings of the IEEE International Conference on Computer Vision Workshops*, pages 0–0, 2019.

[31] Kaiming He, Haoqi Fan, Yuxin Wu, Saining Xie, and Ross Girshick. Momentum contrast for unsupervised visual representation learning. *arXiv preprint arXiv:1911.05722*, 2019.

[32] Kaiming He and Jian Sun. Convolutional neural networks at constrained time cost. In *Computer Vision and Pattern Recognition (CVPR)*, 2015.

[33] Kaiming He, Xiangyu Zhang, Shaoqing Ren, and Jian Sun. Deep residual learning for image recognition. In *Computer Vision and Pattern Recognition (CVPR)*, 2016.

[34] Olivier J Hénaff, Aravind Srinivas, Jeffrey De Fauw, Ali Razavi, Carl Doersch, SM Eslami, and Aaron van den Oord. Data-efficient image recognition with contrastive predictive coding. *arXiv preprint arXiv:1905.09272*, 2019.

[35] Phillip Isola, Daniel Zoran, Dilip Krishnan, and Edward H Adelson. Learning visual groups from co-occurrences in space and time. *arXiv preprint arXiv:1511.06811*, 2015.

[36] Dinesh Jayaraman and Kristen Grauman. Learning image representations tied to egomotion. In *ICCV*, 2015.

[37] Neel Joshi, Wolf Kienzle, Mike Toelle, Matt Uyttendaele, and Michael F Cohen. Real-time hyperlapse creation via optimal frame selection. *ACM Transactions on Graphics (TOG)*, 34(4):1–9, 2015.

[38] Armand Joulin, Kevin Tang, and Li Fei-Fei. Efficient image and video co-localization with frank-wolfe algorithm. In *European Conference on Computer Vision*, pages 253–268. Springer, 2014.

[39] Diederik P Kingma and Jimmy Ba. Adam: A method for stochastic optimization. *arXiv*, 2014.

[40] Shu Kong and Charless Fowlkes. Multigrid predictive filter flow for unsupervised learning on videos. *arXiv preprint arXiv:1904.01693*, 2019.

[41] Bruno Korbar, Du Tran, and Lorenzo Torresani. Cooperative learning of audio and video models from self-supervised synchronization. In *Advances in Neural Information Processing Systems*, 2018.

[42] Zihang Lai, Erika Lu, and Weidi Xie. Mast: A memory-augmented self-supervised tracker. *arXiv preprint arXiv:2002.07793*, 2020.

[43] Zihang Lai and Weidi Xie. Self-supervised learning for video correspondence flow. *arXiv preprint arXiv:1905.00875*, 2019.

[44] Xueting Li, Sifei Liu, Shalini De Mello, Xiaolong Wang, Jan Kautz, and Ming-Hsuan Yang. Joint-task self-supervised learning for temporal correspondence. In *Advances in Neural Information Processing Systems*, pages 317–327, 2019.

[45] Yin Li, Manohar Paluri, James M. Rehg, and Piotr Dollár. Unsupervised learning of edges. In *CVPR*, 2016.

[46] Jonathan Long, Evan Shelhamer, and Trevor Darrell. Fully convolutional networks for semantic segmentation. In *CVPR*, 2015.

[47] William Lotter, Gabriel Kreiman, and David Cox. Deep predictive coding networks for video prediction and unsupervised learning. *arXiv preprint arXiv:1605.08104*, 2016.

[48] Bruce D Lucas and Takeo Kanade. An iterative image registration technique with an application to stereo vision. *IJCAI*, 1981.

[49] Jonathon Luiten, Paul Voigtlaender, and Bastian Leibe. Premvos: Proposal-generation, refinement and merging for video object segmentation. In *Asian Conference on Computer Vision*, pages 565–580. Springer, 2018.

[50] Zelun Luo, Boya Peng, De-An Huang, Alexandre Alahi, and Li Fei-Fei. Unsupervised learning of long-term motion dynamics for videos. 2017.

[51] K. K. Maninis, S. Caelles, Y. Chen, J. Pont-Tuset, L. Leal-Taixé, D. Cremers, and L. Van Gool. Video object segmentation without temporal information. *IEEE Transactions on Pattern Analysis and Machine Intelligence*, 41(6):1515–1530, 2019.

[52] Michaël Mathieu, Camille Couprie, and Yann LeCun. Deep multi-scale video prediction beyond mean square error. *arXiv*, 2015.

[53] Marina Meila and Jianbo Shi. Learning segmentation by random walks. In *Advances in neural information processing systems*, pages 873–879, 2001.

[54] Tomas Mikolov, Kai Chen, Greg Corrado, and Jeffrey Dean. Efficient estimation of word representations in vector space. *arXiv preprint arXiv:1301.3781*, 2013.

[55] Ishan Misra, C. Lawrence Zitnick, and Martial Hebert. Shuffle and Learn: Unsupervised Learning using Temporal Order Verification. In *ECCV*, 2016.

[56] Ravi Teja Mullapudi, Steven Chen, Keyi Zhang, Deva Ramanan, and Kayvon Fatahalian. Online model distillation for efficient video inference. In *Proceedings of the IEEE International Conference on Computer Vision*, pages 3573–3582, 2019.

[57] Sourabh A Niyogi and Edward H Adelson. Analyzing gait with spatiotemporal surfaces. In *Proceedings of 1994 IEEE Workshop on Motion of Non-rigid and Articulated Objects*, pages 64–69. IEEE, 1994.

[58] Mehdi Noroozi and Paolo Favaro. Unsupervised learning of visual representations by solving jigsaw puzzles. In *European Conference on Computer Vision*, pages 69–84. Springer, 2016.

[59] Seoung Wug Oh, Joon-Young Lee, Ning Xu, and Seon Joo Kim. Video object segmentation using space-time memory networks. In *Proceedings of the IEEE International Conference on Computer Vision*, pages 9226–9235, 2019.

[60] Aaron van den Oord, Yazhe Li, and Oriol Vinyals. Representation learning with contrastive predictive coding. *arXiv preprint arXiv:1807.03748*, 2018.

[61] Andrew Owens and Alexei A Efros. Audio-visual scene analysis with self-supervised multisensory features. In *Proceedings of the European Conference on Computer Vision (ECCV)*, pages 631–648, 2018.

[62] Andrew Owens, Phillip Isola, Josh McDermott, Antonio Torralba, Edward H Adelson, and William T Freeman. Visually indicated sounds. In *Computer Vision and Pattern Recognition (CVPR)*, 2016.

[63] Deepak Pathak, Ross Girshick, Piotr Dollár, Trevor Darrell, and Bharath Hariharan. Learning features by watching objects move. In *CVPR*, 2017.

[64] F. Perazzi, J. Pont-Tuset, B. McWilliams, L. Van Gool, M. Gross, and A. Sorkine-Hornung. A benchmark dataset and evaluation methodology for video object segmentation. In *Computer Vision and Pattern Recognition*, 2016.

[65] Bryan Perozzi, Rami Al-Rfou, and Steven Skiena. Deepwalk. *Proceedings of the 20th ACM SIGKDD international conference on Knowledge discovery and data mining - KDD '14*, 2014.

[66] Hamed Pirsiavash, Deva Ramanan, and Charless C. Fowlkes. Globally-optimal greedy algorithms for tracking a variable number of objects. In *CVPR 2011*, pages 1201–1208, 2011.

[67] Jordi Pont-Tuset, Federico Perazzi, Sergi Caelles, Pablo Arbeláez, Alexander Sorkine-Hornung, and Luc Van Gool. The 2017 davis challenge on video object segmentation. *arXiv:1704.00675*, 2017.

[68] Deva Ramanan, David A Forsyth, and Andrew Zisserman. Strike a pose: Tracking people by finding stylized poses. In *CVPR*, 2005.

[69] Steven M Seitz and Simon Baker. Filter flow. In *2009 IEEE 12th International Conference on Computer Vision*, pages 143–150. IEEE, 2009.

[70] Pierre Sermanet, Corey Lynch, Yevgen Chebotar, Jasmine Hsu, Eric Jang, Stefan Schaal, Sergey Levine, and Google Brain. Time-contrastive networks: Self-supervised learning from video. In *2018 IEEE International Conference on Robotics and Automation (ICRA)*, pages 1134–1141. IEEE, 2018.

[71] Jianbo Shi and Jitendra Malik. Motion segmentation and tracking using normalized cuts. In *Sixth International Conference on Computer Vision (IEEE Cat. No. 98CH36271)*, pages 1154–1160. IEEE, 1998.

[72] Jianbo Shi and Jitendra Malik. Normalized cuts and image segmentation. *IEEE Transactions on pattern analysis and machine intelligence*, 22(8):888–905, 2000.

[73] Nitish Srivastava, Geoffrey Hinton, Alex Krizhevsky, Ilya Sutskever, and Ruslan Salakhutdinov. Dropout: A simple way to prevent neural networks from overfitting. *The Journal of Machine Learning Research*, pages 1929–1958, 2014.

[74] Nitish Srivastava, Elman Mansimov, and Ruslan Salakhutdinov. Unsupervised learning of video representations using LSTMs. *arXiv*, 2015.

[75] Yu Sun, Xiaolong Wang, Zhuang Liu, John Miller, Alexei A. Efros, and Moritz Hardt. Test-time training with self-supervision for generalization under distribution shifts. In *International Conference on Machine Learning (ICML)*, 2020.

[76] Jian Tang, Meng Qu, Mingzhe Wang, Ming Zhang, Jun Yan, and Qiaozhu Mei. Line: Large-scale information network embedding. In *Proceedings of the 24th international conference on world wide web*, pages 1067–1077, 2015.

[77] Yonglong Tian, Dilip Krishnan, and Phillip Isola. Contrastive multiview coding. *CoRR*, abs/1906.05849, 2019.

[78] Hsiao-Yu Tung, Hsiao-Wei Tung, Ersin Yumer, and Katerina Fragkiadaki. Self-supervised learning of motion capture. In *NIPS*, 2017.

[79] Jack Valmadre, Luca Bertinetto, Joao F Henriques, Ran Tao, Andrea Vedaldi, Arnold WM Smeulders, Philip HS Torr, and Efstratios Gavves. Long-term tracking in the wild: A benchmark. In *Proceedings of the European Conference on Computer Vision (ECCV)*, pages 670–685, 2018.

[80] Aäron van den Oord, Yazhe Li, and Oriol Vinyals. Representation learning with contrastive predictive coding. *CoRR*, abs/1807.03748, 2018.

[81] Paul Voigtlaender, Michael Krause, Aljosa Osep, Jonathon Luiten, Berin Balachandar Gnana Sekar, Andreas Geiger, and Bastian Leibe. MOTS: multi-object tracking and segmentation. *CoRR*, abs/1902.03604, 2019.

[82] Paul Voigtlaender and Bastian Leibe. Online adaptation of convolutional neural networks for video object segmentation. *arXiv*, 2017.

[83] Carl Vondrick, Abhinav Shrivastava, Alireza Fathi, Sergio Guadarrama, and Kevin Murphy. Tracking emerges by colorizing videos. In *ECCV*, 2017.

[84] Ning Wang, Yibing Song, Chao Ma, Wengang Zhou, Wei Liu, and Houqiang Li. Unsupervised deep tracking. In *Proceedings of the IEEE Conference on Computer Vision and Pattern Recognition*, pages 1308–1317, 2019.

[85] Qiang Wang, Li Zhang, Luca Bertinetto, Weiming Hu, and Philip HS Torr. Fast online object tracking and segmentation: A unifying approach. In *Proceedings of the IEEE conference on computer vision and pattern recognition*, pages 1328–1338, 2019.

[86] Xiaolong Wang and Abhinav Gupta. Unsupervised learning of visual representations using videos. In *ICCV*, 2015.

[87] Xiaolong Wang, Kaiming He, and Abhinav Gupta. Transitive invariance for self-supervised visual representation learning. In *ICCV*, 2017.

[88] Xiaolong Wang, Allan Jabri, and Alexei A Efros. Learning correspondence from the cycle-consistency of time. In *Proceedings of the IEEE Conference on Computer Vision and Pattern Recognition*, pages 2566–2576, 2019.

[89] Donglai Wei, Joseph Lim, Andrew Zisserman, and William T. Freeman. Learning and using the arrow of time. In *IEEE Conference on Computer Vision and Pattern Recognition*, 2018.

[90] Max Wertheimer. Laws of organization in perceptual forms. In *A source book of Gestalt psychology*, pages 71–88. Routledge & Kegan Paul, London, 1938.

[91] Josh Wills, Sameer Agarwal, and Serge Belongie. What went where. In *IEEE Conference on Computer Vision and Pattern Recognition (CVPR)*, volume 1, pages 37–44, Madison, WI, 2003.

[92] Zhirong Wu, Yuanjun Xiong, Stella X Yu, and Dahua Lin. Unsupervised feature learning via non-parametric instance discrimination. In *Proceedings of the IEEE Conference on Computer Vision and Pattern Recognition*, pages 3733–3742, 2018.

[93] Linjie Yang, Yanran Wang, Xuehan Xiong, Jianchao Yang, and Aggelos K Katsaggelos. Efficient video object segmentation via network modulation. 2018.

[94] Amir Roshan Zamir, Afshin Dehghan, and Mubarak Shah. Gmcp-tracker: Global multi-object tracking using generalized minimum clique graphs. In *European Conference on Computer Vision*, pages 343–356. Springer, 2012.

[95] Lihi Zelnik-Manor and Michal Irani. Event-based analysis of video. In *Proceedings of the 2001 IEEE Computer Society Conference on Computer Vision and Pattern Recognition. CVPR 2001*, volume 2, pages II–II. IEEE, 2001.

[96] Li Zhang, Yuan Li, and Ramakant Nevatia. Global data association for multi-object tracking using network flows. In *2008 IEEE Conference on Computer Vision and Pattern Recognition*, pages 1–8. IEEE, 2008.

[97] Richard Zhang, Phillip Isola, and Alexei A Efros. Split-brain autoencoders: Unsupervised learning by cross-channel prediction. In *Proceedings of the IEEE Conference on Computer Vision and Pattern Recognition*, pages 1058–1067, 2017.

[98] Qixian Zhou, Xiaodan Liang, Ke Gong, and Liang Lin. Adaptive temporal encoding network for video instance-level human parsing. In *ACM MM*, 2018.

[99] Tinghui Zhou, Philipp Krahenbuhl, Mathieu Aubry, Qixing Huang, and Alexei A Efros. Learning dense correspondence via 3d-guided cycle consistency. In *CVPR*, 2016.

A Comparison to Supervised Methods on DAVIS-VOS

The proposed method outperforms many supervised methods for video object segmentation, despite relying on a simple label propagation algorithm, never being trained for object segmentation, and never training on the DAVIS dataset.

Method	Backbone	Train Data (#frames)	$\mathcal{J}\&\mathcal{F}_\text{m}$	$\mathcal{J}_\text{m}$	$\mathcal{J}_\text{r}$	$\mathcal{F}_\text{m}$	$\mathcal{F}_\text{r}$
OSMN [93]	VGG-16	I/C/D (1.2M + 227k)	54.8	52.5	60.9	57.1	66.1
SiamMask [85]	ResNet-50	I/V/C/Y (1.2M + 2.7M)	56.4	54.3	62.8	58.5	67.5
OSVOS [10]	VGG-16	I/D (1.2M + 10k)	60.3	56.6	63.8	63.9	73.8
OnAVOS [82]	ResNet-38	I/C/P/D (1.2M + 517k)	65.4	61.6	67.4	69.1	75.4
OSVOS-S [51]	VGG-16	I/P/D (1.2M + 17k)	68.0	64.7	74.2	71.3	80.7
FEELVOS [81]	Xception-65	I/C/D/Y (1.2M + 663k)	71.5	69.1	79.1	74.0	83.8
PReMVOS [49]	ResNet-101	I/C/D/P/M (1.2M + 527k)	77.8	73.9	83.1	81.8	88.9
STM [59]	ResNet-50	I/D/Y (1.2M + 164k)	81.8	79.2	-	84.3	-
Ours	ResNet-18	K (20M unlabeled)	67.6	64.8	76.1	70.2	82.1

Table 3: **Video object segmentation results on DAVIS 2017 val set**. We show results of state-of-the-art **supervised** approaches in comparison to our unsupervised one (see main paper for comparison with unsupervised methods). Key for *Train Data* column: I=ImageNet, K=Kinetics, V = ImageNet-VID, C=COCO, D=DAVIS, M=Mapillary, P=PASCAL-VOC Y=YouTube-VOS. $\mathcal{F}$ is a boundary alignment metric, while $\mathcal{J}$ measures region similarity as IOU between masks. Note that our method beats half the supervised approaches, despite seeing no labels.

B Using a Single Feature Map

We follow the simplest approach for extracting nodes from an image without supervision, which is to simply sample patches in a convolutional manner. The most efficient way of doing this would be to only encode the image once, and pool the features to obtain region-level features [46].

We began with that idea and found that the network could cheat to solve this dense correspondence task even across long sequences, by learning a shortcut. It is well-known that convolutional networks can learn to rely on boundary artifacts [46] to encode position information, which is useful for the dense correspondence task. To control for this, we considered reducing the receptive field of the network to the extent that entries in the center crop of the spatial feature map do not see the boundary; we then cropped the feature map to only see this region. We also considered randomly blurring frames in each video to combat space-time compression artifacts, as well as considering *random* videos – made of noise. Surprisingly, the network was able to learn a shortcut in each case. In the case of random videos, the shortcut solution was not as successful, but we still found it surprising that the self-supervised loss of Equation 5 could be optimized at all.

C Additional Ablation

Effect of frame-rate at training time We ablate the effect of frame-rate (i.e. frames per second) used to generate sequences for training, on downstream object segmentation performance. The case of infinite frame-rate corresponds to the setting where the *same* image is used in each time step; this experiment is meant to disentangle the effect of data augmentation (spatial jittering of patches) from the natural "data augmentation" observed in video. We observe that spatio-temporal transformation is beneficial for learning of representations that transfer better for object segmentation.

Frame rate	$\mathcal{J}\&\mathcal{F}_\text{m}$
2	65.9
4	67.5
8	67.6
30	62.3
∞	57.5

D Hyper-parameters

We list the key hyper-parameters and ranges considered at training time. We did not tune the patch extraction strategy and the majority of hyper-parameters. The hyper-parameters varied, namely edge dropout and video length, were ablated in Section 3 (shown in bold). Note that the training path length is twice that of the video sequence length (since we construct a palindrome).

- Learning rate: {0.0001}
- Temperature τ: {0.07}
- Dimensionality d of embedding: {128}
- Frame size: {256}
- Video length: **{2, 4, 6, 10}**
- Edge dropout: **{0, 0.1, 0.2, 0.3}**
- Frame rate: **{2, 4, 8, 30}**
- Patch Size: {64}
- Patch Stride: {32}
- Spatial Jittering (crop range): {(0.7, 0.9)}

Hyper-parameters for Label Propagation (Test): Here, bold denotes setting used in experiments.

- Temperature: {0.07} (same as training)
- Number of neighbors: {**10**, 20}
- Number of context frames: {varies per task}
- Radius on feature map considered for source nodes: {**12**, 20}

E Test-time Training Details

We adopt the same hyper-parameters for optimization as in training: we use the Adam optimizer with learning rate 0.0001. Given an input video I, we fine-tune the model parameters by applying Algorithm 1 with input frames $\{I_{t-m}, ..., I_t, ..., I_{t+m}\}$, *prior* to propagating labels to I_t. For efficiency, we only finetune the model every 5 timesteps, applying Adam for 100 updates. In practice, we use $m = 10$, which we did not tune.

F Utility Functions used in Algorithm 1

Algorithm 2 Utility functions.

```
// psize : size of patches to be extracted

import torch
import kornia.augmentation as K

# Turning images into list of patches
unfold = torch.nn.Unfold((psize, psize), stride=(psize//2, psize//2))

# l2 normalization
l2_norm = lambda x: torch.nn.functional.normalize(x, p=2, dim=1)

# Slightly cropping patches once extracted
spatial_jitter = K.RandomResizedCrop(size=(psize, psize), scale=(0.7, 0.9), ratio=(0.7, 1.3))
```